Dissipative particle dynamics study on the morphology changes of diblock copolymer lamellar microdomains due to steady shear

Wei Liu, Hu-Jun Qian, Zhong-Yuan Lu,* Ze-Sheng Li, and Chia-Chung Sun
State Key Laboratory of Theoretical and Computational Chemistry, Institute of Theoretical Chemistry, Jilin University, Changchun 130023, China

(Received 31 December 2005; revised manuscript received 14 March 2006; published 9 August 2006)

The morphology changes of linear diblock copolymer lamellar microdomains under uniform simple shear are studied via the dissipative particle dynamics technique. The parallel and perpendicular reorientations of the lamellae are observed in the simulations, and two different reorientation mechanisms, under small and large shear rates respectively, are proposed. The parallel-to-perpendicular transition is also observed and the kinetics is discussed. Sinusoidal and chevron instabilities due to the shear are found. After relaxation the peculiar "bidirectionally undulating" instability is obtained.

DOI: 10.1103/PhysRevE.74.021802 PACS number(s): 61.25.Hq, 61.41.+e, 64.75.+g

I. INTRODUCTION

Block copolymers are macromolecules composed of sequences of chemically distinct and mutually incompatible monomers that are covalently bonded. They tend to form various ordered morphologies which are in general on the nanometer scale through self-assembly and microphase separation. This is a desirable property in research areas such as supramolecular chemistry, materials science, and nanotechnology. The morphologies of block copolymers can be systematically controlled by carefully choosing the polymer segments (the Flory-Huggins interaction parameter χ), the chain length (the degree of polymerization N), and the composition (the monomer volume fraction f). Thus block copolymers have become the model molecules in the above-mentioned disciplines and have attracted intensive theoretical and experimental attention [1–5].

Diblock copolymers, which are block copolymers composed of only two distinct types of monomers, in particular, have attracted considerable research activities due to their inherent simplicity. Classical equilibrium microstructures such as lamellae (LAM), hexagonally packed cylinders (HEX), and spheres positioned on body-centered-cubic lattice (bcc) have been identified experimentally and predicted theoretically for quite a long time. Recently, hexagonally modulated lamellae (HML), hexagonally perforated layers (HPL), and bicontinuous $Ia\bar{3}d$ gyroid (G) were discovered. Among these many phases, lamellar phase is the most studied one.

The behavior of lamellae under shear flow is of great interest to both scientists and engineers. Shear can be used to change the orientation of the microphases and to obtain globally aligned structures. Three orientations have been observed under various conditions: the parallel (i.e., the lamellar normal is parallel to the velocity gradient direction), the perpendicular (in which the lamellar normal is parallel to the vortex direction), and the transverse orientation (that is, the lamellar normal is parallel to the velocity direction) which is usually a transient nonequilibrium state [6–11]. However, the fundamental understanding on the mechanism of the selection of one orientation over the other, the dynamics of the interconversion between these orientations, and the detailed influence induced by shearing still remains unraveled. It is worth pointing out that *in situ*, time-resolved experiments are providing insightful information on the actual processes of the structural evolution that can occur during flow-induced alignment of ordered block copolymers [11–14].

Due to the spectacular increase in computing power over recent years, computer simulation has become a powerful tool to investigate the behavior and properties of complex macromolecular systems [15–18]. The Monte Carlo [19] method can be adopted to study the equilibrium properties of such systems in an acceptable amount of computer time. Recently, the dynamic density functional method [20–22], time-dependent Ginzburg-Landau (TDGL) method [23,24], and cell dynamical method [25–27] had been developed to study the dynamics of complex polymer systems. Molecular dynamics can be a more appropriate method of the study of nonequilibrium properties. However, the simulation of polymers at the atomistic scale is a very demanding task because of the large length scale and the wide range of time scales. Therefore, coarse-grained methods have been developed in an attempt to reduce the complexity of the atomistic simulation model. For example, Guo, Kremer, and Soddemann [28] used a coarse-grained model successfully to study the shear-induced alignment of amphiphilic systems by nonequilibrium molecular dynamics. Among those various methods, the dissipative particle dynamics (DPD) [29–33] is a promising technique for the modeling of the rheology and morphology of complex liquids. DPD uses rather soft particles (beads) which represent a cluster of atoms, to simulate fluids on a mesoscopic scale. This reduces the number of particles taken into account and permits a large integration time step. Furthermore, by incorporating the momentum-conserving stochastic thermostat and satisfying the fluctuation-dissipation theorem (based on the work by Español and Warren [31]), the DPD technique can produce a well-defined canonical (NVT) ensemble and can reproduce momentum propagation correctly, which is often quite important in the dynamics of complex fluids. Block copolymers can be simulated with this technique by linking DPD beads together with entropy

*Corresponding author. Email address: luzhy@mail.jlu.edu.cn

springs [34,35]. Groot and Madden [36] had successfully used this method to study the microphase separation of linear diblock copolymers, the results are consistent with those predicted by mean field theory. Inspired by their pioneering work, and being aware of the significance of the shear flow in the industrial processing, we study the behavior of linear diblock copolymers under homogeneous simple shear via the DPD technique.

II. DPD IN MORE DETAIL AND MODEL CONSTRUCTION

In the DPD method, the force experienced by particle i is composed of three parts: a conservative force $\mathbf{F}^C$, a dissipative force $\mathbf{F}^D$, and a random force $\mathbf{F}^R$. To model the block copolymers, we tie the adjacent beads in a single polymer chain by harmonic spring force $\mathbf{F}^S$. Each force is pairwise additive:

$$\mathbf{f}_i = \sum_{j \neq i} (\mathbf{F}_{ij}^C + \mathbf{F}_{ij}^D + \mathbf{F}_{ij}^R + \mathbf{F}_{ij}^S), \tag{1}$$

where the sum runs over all other particles within a certain cutoff radius r_c to speed up the force calculation.

The conservative force is a soft repulsion acting along the line of centers and is determined by

$$\mathbf{F}_{ij}^C = \begin{cases} \alpha_{ij}(1 - r_{ij}/r_c)\hat{\mathbf{r}}_{ij} & (r_{ij} < 1), \\ \mathbf{0} & (r_{ij} \geqslant 1), \end{cases} \tag{2}$$

where α_{ij} is a maximum repulsion between particle i and particle j; $\mathbf{r}_{ij}=\mathbf{r}_i-\mathbf{r}_j$, $r_{ij}=|\mathbf{r}_{ij}|$, and $\hat{\mathbf{r}}_{ij}=\mathbf{r}_{ij}/|\mathbf{r}_{ij}|$. The number density of our model is three. The repulsion parameter is then related to the Flory-Huggins χ-parameter by:

$$\alpha_{ij} \approx \alpha_{ii} + 3.27\chi_{ij} \quad (\rho = 3), \tag{3}$$

where the interaction parameter between the same bead type α_{ii} equals 25 to correctly describe the compressibility of water [32]. We are trying to deal with a general model system; water is a suitable representative of liquids for this purpose because its compressibility is larger than other liquids and the values do not differ significantly.

The dissipative force and the random force are given by

$$\mathbf{F}_{ij}^D = -\zeta\omega^D(r_{ij})(\hat{\mathbf{r}}_{ij} \cdot \mathbf{v}_{ij})\hat{\mathbf{r}}_{ij}, \quad \mathbf{F}_{ij}^R = \sigma\omega^R(r_{ij})\frac{\xi_{ij}}{\sqrt{\Delta t}}\hat{\mathbf{r}}_{ij}, \tag{4}$$

where ζ is the friction constant which controls the extent of heat dissipation in a time step. (Note that the negative sign in front of ζ indicates that the dissipative force is opposite to the relative velocity $\mathbf{v}_{ij}$ thus in effect dissipates the heat.) σ is the noise strength which controls the energy pumped into the system in a time step. ω^D and ω^R are r-dependent weight functions vanishing for $r > r_c = 1$, $\mathbf{v}_{ij}=\mathbf{v}_i-\mathbf{v}_j$, and ξ_{ij} is a random number with zero mean and unit variance. These two forces also act along the line of centers and conserve linear as well as angular momentum. Note that there is an independent random function for each *pair* of particles. To correctly produce the canonical ensemble, it has been proven [30] that the following relation should hold:

$$\omega^D(r) = [\omega^R(r)]^2, \quad \sigma^2 = 2\zeta k_B T. \tag{5}$$

The dissipative force and the random force, when coupled through the above relations, can act as a thermostat. To make things simple, we also choose [32]

$$\omega^D(r) = [\omega^R(r)]^2 = \begin{cases} (1-r)^2 & (r < 1), \\ \mathbf{0} & (r \geqslant 1), \end{cases} \tag{6}$$

and $\sigma=3.67$. The bond force is

$$\mathbf{F}_{ij}^S = C\mathbf{r}_{ij} \tag{7}$$

when bead i is directly bonded to bead j. The parameter C is set to be 4.0.

The time evolution of the particles is governed by the classic Newton's equations of motion

$$\frac{d\mathbf{r}_i}{dt} = \mathbf{v}_i, \quad \frac{d\mathbf{v}_i}{dt} = \mathbf{f}_i. \tag{8}$$

The integration scheme used here is based on the modified velocity Verlet algorithm according to Groot and Warren [32]. For easy numerical handling, we have chosen the cutoff radius, the particle mass, and the temperature as follows

$$r_c = m = kT = 1. \tag{9}$$

As a consequence, our unit of time τ is

$$\tau = r_c\sqrt{m/kT}. \tag{10}$$

The time step is 0.06 in DPD time unit which is a tradeoff between good temperature control and possible maximum time step size. Recent studies [37,38] imply that, in ordered microphases which consist of DPD beads that are connected by springs, artifacts may appear if a relatively large time step such as 0.06 is employed. Under nonequilibrium conditions the artifacts are supposed to become even more pronounced. Following Ref. [37], we have performed additional simulations with time step 0.06 to examine the spatial variations of the kinetic temperatures of different bead types. However, we have not found any significant spatial variations. Furthermore, we have checked the effects of different time increment sizes on the space-resolved normal pressure profile of the layered system with $f=0.5$ and $\chi N = 46$. The artifacts do exist for a time step 0.06 as the deviations of the normal pressure profile from the constant "bulk" value are observed. To ensure that such artifacts do not affect our observations and conclusions of the morphological behavior of the simulated diblock copolymer systems under shear, we use a smaller time step (0.03) to perform some additional simulation runs in the cases of the parallel reorientation, the parallel-perpendicular reorientation, the double undulation, and so on, whose definition will appear in the following discussion. The morphological behavior is the same as that we have obtained using time step 0.06. Therefore, we still choose 0.06 as the time increment for saving the computation time to the maximum.

The selection of the parameters mentioned above which define the model, such as σ, ζ, and C, is mainly in accordance with Refs. [32,36] since our purpose is to study the general model that used in DPD method.

There are several methods to model shear flows [29,39–41]. In this study, we used the Lees-Edwards periodic boundary conditions (PBC) [15,42] to set up and maintain a steady linear velocity profile with gradient $\dot{\gamma}=dv_x/dr_y$. The planar shear flow profile is

$$\mathbf{u} = \dot{\gamma} y \mathbf{i}_x. \tag{11}$$

The flow direction is parallel to the X axis, the velocity gradient is along the Y direction, and the Z axis represents the vortex direction. $\mathbf{u}$ is the flow velocity vector, and $\mathbf{i}_x$ is the unit vector in the flow direction. Care must be taken that the Reynolds number of the system should not be too large, otherwise microturbulence may occur and the system becomes unstable [43].

A box of size $20\times20\times20$ is simulated with Lees-Edwards PBC. Thus in total 24 000 beads are present in the box. The beads can be assigned of type A or type B on demand before the simulation starts so as to study different systems of different compositions. The number of beads in a single block copolymer chain is 10, while the composition of the chain may vary. We use A_mB_n to indicate a block copolymer chain composed of m A beads and n B beads. The composition fraction of bead A is thus determined by $f=m/(m+n)$.

In computer simulations of lamellar systems, the dimension in the normal of the layer should be at least larger than two layer-spacings in order to obtain reliable results. In most of our simulations, the periodicity is 3. It is argued that the box size with $20\times20\times20$ may not be large enough to obtain quantitatively accurate measurements. For computational efficiency, our simulations are run at a fixed volume and aspect ratio, as a result the box is likely to create finite size effects as its dimension may not be compatible with the equilibrium layer spacing. In order to obtain an estimation of the finite size effects, we perform some additional simulations with varied box dimensions and aspect ratio on a parallel lamellar system with $f=0.5$ and $\chi N=46$. A perfect equilibrium, tensionless lamellar system should possess equal global averages of the pressure tensor diagonal components, i.e., $P_{xx}=P_{yy}=P_{zz}$ [44]. These values, however, in our case ($20\times20\times20$ box) are $P_{xx}=21.569$, $P_{yy}=21.520$, and $P_{zz}=21.568$. That is, $P_{xx}=P_{zz}>P_{yy}$ which indicates that the layer system is under dilatation. This is due to the incompatibility between the layer spacing and the box geometry. Therefore we compress the simulation box in the dilated direction (the Y direction) and expand the box in the other two directions, at the same time, we keep the volume constant. We find that when the length of the box in the Y direction, L_y, is 97.9% of the original value, $P_{xx}=P_{zz}=P_{yy}$. The deformation is not quite large. As our goal is the study of morphological changes associated with the shearing process, the finite size effects are not likely to strongly affect our results and conclusions. Furthermore, as a recent study shows [45], when purely repulsive conservative potential is used, finite size effects are not severe for a system as large as, say, $20\times20\times20$.

III. SIMULATION RESULTS AND DISCUSSION

We have studied diblock copolymers with different compositions (from $f=0.3$ to $f=0.5$). The LAM structures are obtained by changing χN over a certain value. In order to observe the response of these structures to the relatively weak, intermediate, and strong shear flows, we have set the shear rates to 0.001, 0.01, 0.1, and 0.2 in reduced units, respectively. The choice of these values are based upon our experience rather than theoretical deduction, as these shear rates can lead to different phenomena and to our knowledge there is no satisfactory theory in DPD method yet that can predict which shear rates we ought to choose. To understand the simulation results more directly and intuitively, we visualize the output data by plotting the isodensity surface of the monomer A. The isodensity value is 1.5.

First, we would like to point out a common observation in our simulations. In every system we have investigated, the application of shear dramatically accelerates the evolution of the system to the final structure when the shear rate is sufficiently large (in our simulations the threshold is of the magnitude of 0.0001). Generally speaking, it usually takes tens or even hundreds of thousands time steps for a system to reach the final equilibrium state without shear. When the shear is applied, however, the system can achieve the final steady structure faster by one to several orders of magnitude depending on the applied shear rate, and the final structure is oriented by the flow. This effect implies the application of shear flow in industrial block copolymer processing to speed up the formation of desired globally aligned ordered structures. In the following we begin to focus on two interesting shear effects.

A. Shear-induced reorientation

Over the last decades a large number of experiments had been performed on the reorientation behavior of LAM structures under various shear flows. For a review, see Hamley [46]. It is now clear that large amplitude oscillatory shear (LAOS) at different frequencies can be used to produce either a parallel or perpendicular alignment of a diblock copolymer lamellar phase. Recently, Leist *et al.* [47] showed that the reorientation can be described as a function of the shear rate rather than as a function of the oscillatory frequency. We thus use the simple steady shear in our simulations. Koppi *et al.* [9] found that both parallel and perpendicular orientations could be accessed in a poly(ethlene-propylene)-poly(ethylethylene) (PEP-PEE) diblock system depending on the shear rate and temperature. They speculated that lamellar undulations caused by the vorticity of the shear field would cause the parallel alignment to be unstable relative to the perpendicular alignment. They also found that the perpendicular orientation could be obtained by shearing an already parallel-oriented system at a higher shear rate, but the reverse process was not observed. Kornfield and coworkers used birefringence measurements on a nearly symmetric poly(styrene)-poly(isoprene) (PS-PI) diblock system sheared in real time [48]. They found that at high frequencies a parallel orientation was obtained, while at lower frequencies they obtained the perpendicular orientation. In either

case, a relatively fast process took place first then followed by a slow process. The fast process was the depletion of lamellae in the transverse orientation when forming the ultimate perpendicular orientation and the depletion of perpendicular lamellae when forming the ultimate parallel structure. Generally speaking, however, in experiments it is not known in advance which orientation (parallel or perpendicular) is preferred for a specific system.

We have prepared a randomly oriented LAM structure with $f=0.5$ and $\chi N=46$, at which the system is away from both weak and strong segregation limits. (In fact we have prepared several randomly oriented LAM with different orientations relative to the simulation box and let them undergo reorientation. The results are the same.) Then steady shears of various shear rates 0.001, 0.01, and 0.2 are applied, respectively. For each shear rate, we evolve the system until a final stable state is achieved. Under the relatively small ($\dot{\gamma}=0.001$), as well as the intermediate shear rates (for example $\dot{\gamma}=0.01$), the lamellae take the parallel orientation, while under the strong shear ($\dot{\gamma}=0.2$) perpendicular orientation is observed. The morphological changes during the reorientation processes subject to different shear rates are contrasting. When the shear rate is rather small, it seems that the lamellar structure is largely retained (see Fig. 1). After some thousand time steps, the layers as a whole gradually reorientate so as to take the parallel orientation [Fig. 1(b)]. It looks like that the shear flow is "rotating" the layers while the layers are still intact. Deformations can take place along with the reorientation process [Fig. 1(c)]. Neighboring layers may be linked at some regions by interlayer rodlike microdomains [(Fig. 1(d))]. Finally, when the lamellae have aligned perfectly in parallel with the shear plane, the microdomains between the adjacent layers disappear, and the flat lamellar structures are recovered [Fig. 1(e)].

When the shear rate is quite large, however, it appears to us that the reorientation process can be divided into two stages (see Fig. 2). At the first stage, the strong shear flow destroys the lamellar layers completely, the flat layers disappear, and the microdomains are totally disordered along the gradient and vortex axes. Note that even in this quite disordered state, due to the strong shear rate, the microdomains are somewhat orientated. That is, the microdomains are aligned to the flow direction. This breakup process is very fast, within several thousand time steps. At the second stage, as the thermodynamics of this system favors the lamellar structure, the microdomains begin to reform the LAM structure and the shear flow induces the structure to be perpendicularly oriented, i.e., the lamellae reformation process and the reorientation process proceed concurrently. However, a satisfactory interpretation of the preference of the perpendicular orientation over the parallel one, is still needed to be thoroughly studied. This second process is relatively slower than the preceding one, but is still much faster than the zero shear rate case. We find that the critical shear rate above which the LAM is perpendicularly oriented is around 0.2. If the shear rate is much larger than this value, the temperature of the system becomes unstable. This indicates the presence of artifacts introduced by the Lees-Edwards boundary conditions. The energy introduced by the Lees-Edwards boundary condition when particles cross the XY plane at $Z=-10$ or

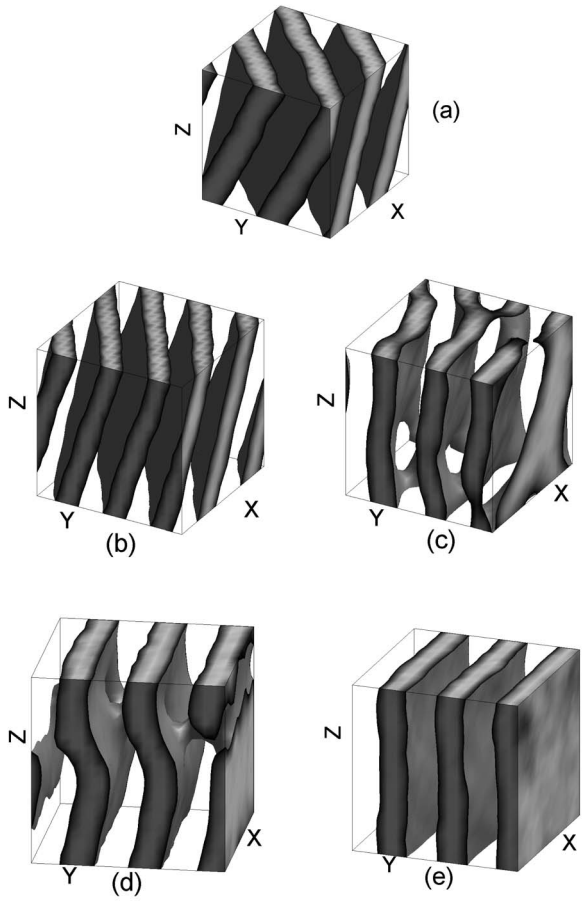

FIG. 1. Snapshots of the system under shear. $\dot{\gamma}=0.001$, $f=0.5$, $\chi N=46$. (a) is the original randomly oriented lamellae. (b)–(e) are snapshots taken at every 10 000 time steps. The box is of dimension $20\times20\times20$.

$Z=10$ is too large to be effectively dissipated by the thermostat. Thus the systems with shear rates much larger than 0.2 are likely to produce unreliable results. Consequently we set 0.2 as the highest acceptable shear rate in this study. Beneath this shear rate, the temperature of the system is well controlled and other properties such as pressure, order parameter, mean square end-to-end distances behave normally.

When we apply the strong shear with rate $\dot{\gamma}=0.2$ to the parallel-oriented system which is obtained previously by the application of the weak shear with $\dot{\gamma}=0.001$, a direct parallel-to-perpendicular transition occurs (Fig. 3).

The whole process looks like the layers are forced to distort, so large amplitude local dislocations occur. Adjacent layers can become interconnected through the combination of their local dislocations. Layers are greatly deformed during this process, but are not destroyed, which can be further identified later through careful examination of the time evolution of the order parameter of the system. The interwound layers then evolve into the final perpendicular orientation. It

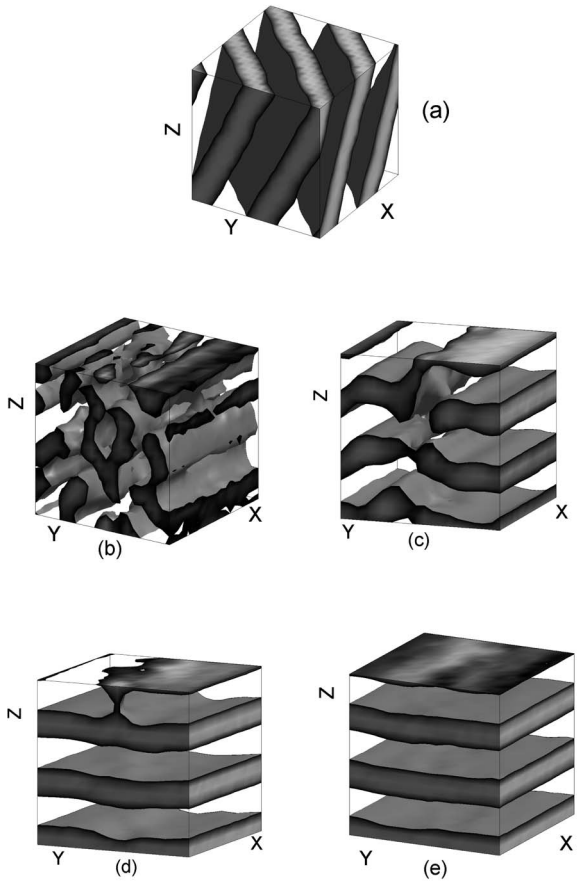

FIG. 2. Snapshots of the system under shear. $\dot{\gamma}=0.2$, $f=0.5$, $\chi N=46$. (a) is the original randomly oriented lamellae. (b)–(e) are snapshots taken at every 5000 time steps. The box is of dimension $20\times20\times20$.

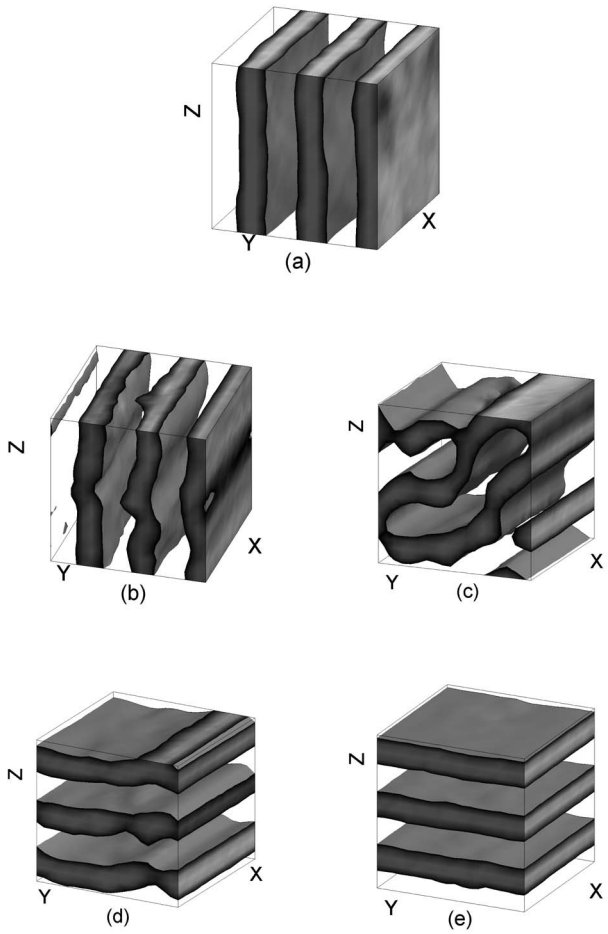

FIG. 3. Snapshots of the system under shear. $\dot{\gamma}=0.2$, $f=0.5$, $\chi N=46$. (a) is the parallel oriented lamellae. (b)–(e) are snapshots taken at every 5000 time steps. The box is of dimension $20\times20\times20$.

is clear now, that in such DPD model systems which are near the weak segregation limit, the perpendicular orientation is the favored orientation under high shear rates.

It is worth a further consideration here. The shear rate is 0.2, which is identical to the one that we have used to perpendicularly reorient the randomly oriented lamellae. In the latter case, layer breakup takes place (Fig. 2). But in this parallel-to-perpendicular transition the layer breakup does not occur. The reason may be that the lamellae are already aligned previously by the weak shear and parallel oriented, the interactions between the flow and the layers have been greatly reduced by the adoption of the parallel orientation. Therefore the flow is not able to break up the layers. The application of strong shear to the perpendicular oriented lamellae, however, seems unable to cause the transition to the parallel one.

Besides the snapshots of the systems, we have monitored the structural evolution of these systems with $f=0.5$, $\chi N=46$ as functions of shear rate and time by the time-resolved orientational order parameter (Fig. 4) measured by the Saupe tensor [49]

$$Q_{\alpha\beta}=\frac{3}{2}\left(\hat{r}_\alpha\hat{r}_\beta-\frac{1}{3}\delta_{\alpha\beta}\right). \tag{12}$$

Here, $\hat{\mathbf{r}}$ is a unit vector directing along the bond which connects the A block and the B block in a single diblock, i.e., the bond is confined to the interface. The characters α and β are Cartesian indices, δ is the Kronecker symbol. The largest eigenvalue of the volume average of $Q_{\alpha\beta}$, S, is the order parameter. S is zero in the completely disordered state, and it should be one if the system is perfectly aligned.

We start from the configuration of Fig. 1, that is, randomly oriented lamellae, then perform two simulations, with the shear rates being 0.001, 0.2, respectively. We are familiar with these two values, since they are exactly the ones we used to carry out the parallel and perpendicular reorientation processes, respectively. The order parameter S of the initial

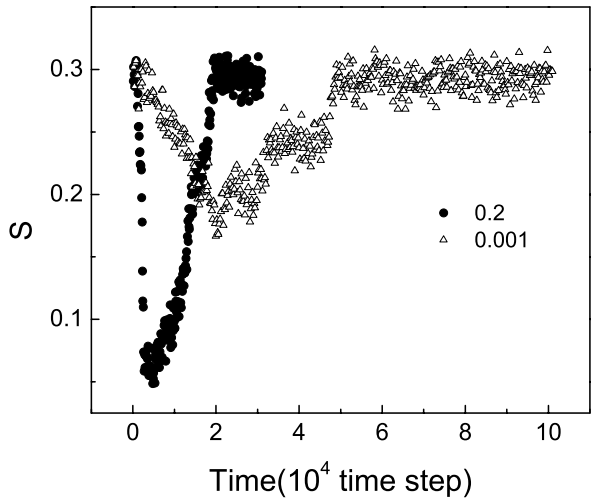

FIG. 4. Order parameter as functions of shear rate and time.

randomly oriented lamellae is around 0.30. In the case of $\dot{\gamma}=0.001$, S gradually goes down. It takes about 20 000 time steps for the system to reach its order parameter minimum, 0.17, approximately. Then, S slowly goes up, finally it restores the initial value, i.e., 0.30. We noted that the minimum is 0.17, which indicates the system still shows some degree of order. It is consistent with our snapshot (c) in Fig. 1. The layers are distorted, but still show layered character. While the shear rate is much larger, $\dot{\gamma}=0.2$, the scene is different. Shearing the lamellae for only about 1000 time steps makes the system nearly completely disordered. It is a quite steep drop, especially compared to the former case. The minimum is 0.05. The system then evolves into lamellae because this is the thermodynamically favorable structure. This process is relatively slow, as it takes about 15 000 time steps or so. After this process, S is 0.3, the typical value for lamellae for this system.

It is noteworthy that the time evolution of S for parallel-perpendicular transition is different from either case mentioned above. S fluctuates around 0.30, without any significant minimum. As we have argued, this may due to the fact that the parallel alignment is already a "frictionless" orientation, any strong interaction between the layers and the flow seems unviable. As a result, the order parameter changes are small.

B. Shear-induced undulations

The undulation instability is commonly encountered when a layered structure is under external stresses [49,50]. Study of such instabilities is extremely well established in structural geology. Undulations in low molecular weight, smectic *A* liquid crystals, have been extensively studied. Wang [51] showed theoretically that undulation instabilities can occur in block copolymers caused by external fields. Shear-induced undulations of block copolymer melts and solutions were also reported [52,53].

Soddemann [54] studied shear-induced undulation via both molecular dynamics simulation and theoretical deduction. When the layers are subject to a shear flow, the normal of the layer will be unaffected as long as the reorientation does not occur. The principal axes of the molecules, however, will tilt due to the flow. The tilt angle, θ, is defined as the angle between the normal of the layer $\hat{n}$ and the direction of the principal molecular axis, $\hat{p}$ [55]. It is this tilt that leads to an effective dilatation of the layers. Consequently, when the effective dilation exceeds a certain value, a layer undulation instability will occur [54,56]. Soddemann *et al.* further found that the tilt angle θ is proportional to the applied shear rate, and the simulated and theoretical predicted critical tilt angle for undulation instability was about 0.18 and 0.35, respectively. We have calculated the tilt angle as a function of shear rate and find that, in this system, the critical shear rate beyond which undulation takes place is about 0.04, and the corresponding tilt angle is about 0.40. We ascribe this rather high value compared to Soddemann's to the soft potential that DPD model used. In spite of this tilt angle difference, however, a linear relationship is also present in our system when the shear rate is between 0.001 and 0.04.

According to Singer [56], without a boundary condition, the sinusoidal instability would appear first above a certain strain threshold. As the strain past the threshold value, the modulation pattern would take the chevron shape. Read *et al.* [57] studied the sinusoidal layer buckling in a block copolymer thermoplastic elastomer and its transition to the chevron with a finite-element technique.

We prepared a system with $f=0.4$ and $\chi N=35$, at which the system is near to the weak segregation limit (WSL). Before applying the shear flow, we have equilibrated the system to a randomly oriented lamellae phase [Fig. 5(a)]. There are some random perforations in the lamellae because the system is near to the WSL. Then steady shears of $\dot{\gamma}=$ 0.001, 0.01, 0.1, and 0.2, respectively, are applied to the system. When the shear rate is relatively small, for example $\dot{\gamma}=0.001$, as can be expected, the lamellae are reoriented to the parallel alignment, though the layers are not quite flat. Unusual phenomenon appears when the shear rate is increased to 0.01. As shown in Fig. 5(b), the parallel oriented lamellae exhibits sinusoidal undulations, which is quite similar to the one that Wang *et al.* discovered [52]. Note that the lamellae normals are confined to the vortex-velocity gradient plane, in accordance with the results of theories [58,59], due to free energy considerations. Interestingly, when this undulation instability is relaxed with the shear flow being turned off for a long enough period of time, a quite strange structure is obtained [Fig. 5(c)]. It is "bidirectionally undulating," that is, the lamellae undulate both in the vortex-velocity gradient plane and the velocity gradient-velocity plane. We attribute this strange undulation instability as the consequence of the previous undulation instability and this phase is a metastable state lying in the pathway from the undulated to the flat lamellae. When the shear is off, the sinusoidally shaped layers try to relax themselves to a stable state. It is obvious that the most stable structure of this system is LAM. But before reaching this structure, the system is trapped into the metastable bidirectionally undulating structure. When the shear is turned on again, the layers return back to the sinusoidal shape. As a test for our speculation, we apply a relatively small shear with $\dot{\gamma}=0.001$ to the bidirectionally undulating system. The flat lamellae are restored. The weak shear flow

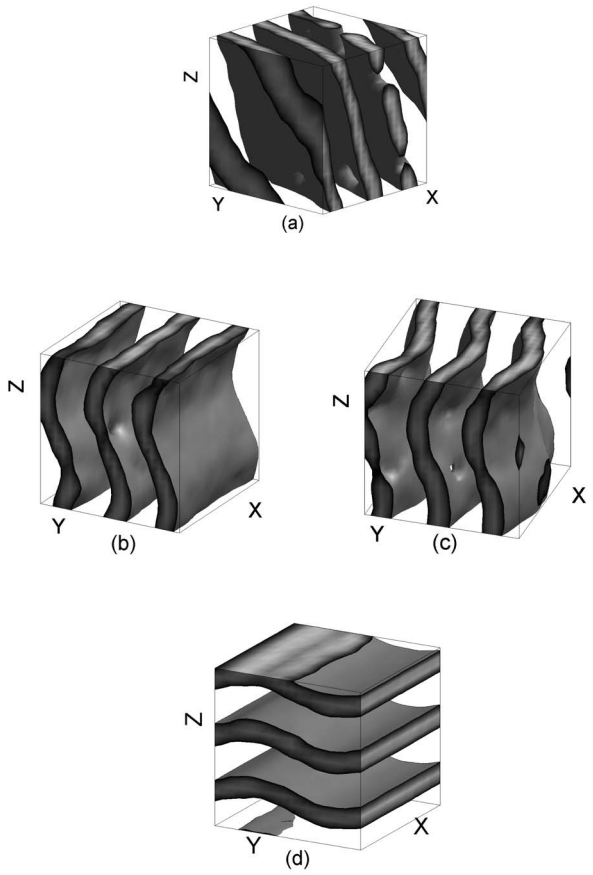

FIG. 5. Snapshots of the system under shear. $\dot{\gamma}=0.2$, $f=0.4$, $\chi N=35$. (a) is the original randomly oriented lamellae. (b) is the sinusoidal undulation. (c) is the bidirectional undulation. The box is of dimension $20\times20\times20$.

seems effective enough to help the system overcoming the free energy barrier to achieve the stable lamellar structure.

Though undulating, the layers still look like they are aligned parallel. We also find that defects may exist. When the shear is stronger further, i.e., $\dot{\gamma}=0.1$, nothing strange happens, the final state is with flat lamellar structure. As we have described above, weak shear seems only to reorientate the lamellae, while intermediate shear is likely to induce undulation instability, and strong shear can lead to suppression of undulation and produce quite flat lamellar layers. Surprisingly, when the shear rate gets even larger, that is, $\dot{\gamma}=0.2$, the sinusoidal undulation emerges again [Fig. 5(d)] but with a perpendicular orientation.

We have simulated a system with $f=0.5$ and $\chi N=150$, i.e., the system is in the strong segregation limit (SSL). Fig. 6(a) shows the equilibrium morphology of this system without shear. When the shear rate is equal to 0.2, we encounter the "chevron" undulation instability [Fig. 6(b)]. We thus speculate that, in DPD models, it is relatively more likely for the lamellae to exhibit chevron undulation in the SSL, while in the weak segregation limit (WSL), the sinusoidal undulation can take place. Relaxation without shear of the chevron for a quite long time again leads to the bidirectional undulation [Fig. 6(c)]. It implies that the bidirectional-undulation

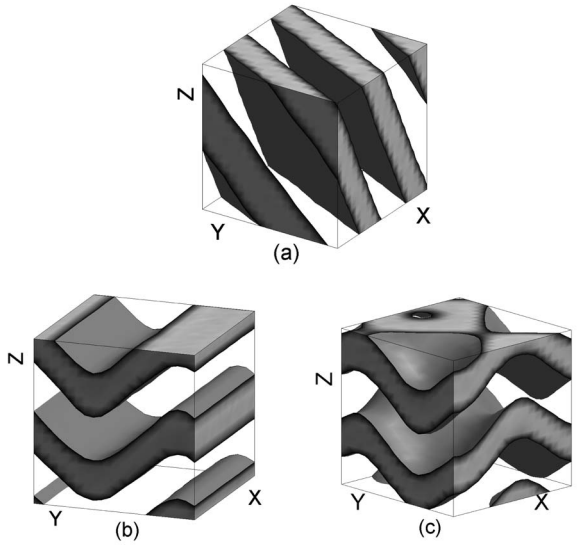

FIG. 6. Snapshots of the system under shear. $\dot{\gamma}=0.2$, $f=0.5$, $\chi N=150$. (a) is the original randomly oriented lamellae. (b) is the chevron structure. (c) is the bidirectional undulation. The box is of dimension $20\times20\times20$.

instability may be universal in these circumstances. In Singer's work on the buckling induced by dilative strain [56], similar bidirectional buckling patterns are predicted.

IV. CONCLUSIONS

In this study, we use the DPD technique to explore the morphology variations of the lamellar phase of linear diblocks under various strengths of simple shears. The parallel and perpendicular reorientation phenomena reported by many researchers have been successfully reproduced in our simulations. By taking the inherent advantages of computer simulations, we can take snapshots of the system of interest at any time during the evolution of the system under shear. That is to say, we can do "real-time" tracing of the evolution of the system. By analyzing the snapshots, as well as the time evolution of the order parameters, we suggest two different mechanisms as to how reorientations of the lamellae take place under weak and strong shears, respectively. In the low shear rate case, the layered structure is always retained, the reorientation is achieved via layer rotation. On the other hand, when the shear rate is large, the layers are completely destroyed, the reorientation is accomplished through a two-step process: a very fast layer breakup process followed by a relatively slow thermodynamics-driven lamellar reformation process. The critical shear rate beyond which the shear is perpendicularly orienting is found generally to be about 0.2, though it may vary from system to system. The parallel to perpendicular orientation process is believed to be via a different path.

The sinusoidal as well as chevron instabilities are identified. When relaxed, bidirectional undulation can occur. Available theories on these phenomena are mostly based on

an energy minimization approach. Our study is mainly targeted to validate the DPD technique, combined with the Lees-Edwards periodic boundary conditions, as a promising tool for the mesoscopic simulations of block copolymer microphase separation behavior under shear. As we have shown in this paper, many interesting, important phenomena associated with block copolymer microphase separation under nonequilibrium conditions which had been well identified in numerous experiments, have been satisfactorily reproduced in our model. However, due to its characteristic soft potential, as well as some other subtle differences, from traditional molecular dynamics methods, for example, the incorporation of stochastic forces, a direct quantitative match of results from DPD and MD may be hard to achieve.

In this study, we implement the steady simple shear. Various patterns of shear flows, for example, oscillatory and reciprocating shears, may lead to rather different results. The effects of shears on other microphases of block copolymers such as hexagonally packed cylinders and body-centered-cubic spheres, and the relation between block copolymer structure and the morphology variation during shear, require further endeavors.

ACKNOWLEDGMENTS

This work is supported by the NSFC (Contract Nos. 20490220, 20404005) and JLSTP (20050562). W.L. and H.J.Q. the Graduate Innovation Lab of Jilin University for their support.

[1] F. S. Bates and G. H. Fredrickson, Annu. Rev. Phys. Chem. **41**, 525 (1990).
[2] G. H. Fredrickson and F. S. Bates, Annu. Rev. Mater. Sci. **26**, 501 (1996).
[3] L. Leibler, Macromolecules **13**, 1602 (1980).
[4] I. W. Hamley, *The Physics of Block Copolymers* (Oxford University Press, Oxford, 1998).
[5] M. Lee, B. K. Cho, and W. C. Zin, Chem. Rev. (Washington, D.C.) **101**, 3869 (2001).
[6] J. Dlugosz, M. J. Folkes, and A. Keller, J. Polym. Sci., Polym. Phys. Ed. **11**, 929 (1973).
[7] M. J. Folkes and A. Keller, J. Polym. Sci., Polym. Phys. Ed. **14**, 833 (1976).
[8] U. Wiessner, Macromol. Chem. Phys. **198**, 3319 (1997).
[9] K. A. Koppi, M. Tirrell, F. S. Bates, K. Almdal, and R. H. Colby, J. Phys. Radium **2**, 1941 (1992).
[10] K. A. Koppi, M. Tirrel, and F. S. Bates, Phys. Rev. Lett. **70**, 1449 (1993).
[11] R. M. Kannan and J. A. Kornfield, Macromolecules **27**, 1177 (1994).
[12] V. K. Gupta, R. Krishnamoorti, J. A. Kornfield, and S. D. Smith, Macromolecules **29**, 1359 (1996).
[13] Y. Zhang and U. Wiesner, J. Chem. Phys. **103**, 4784 (1995).
[14] Z. R. Chen, A. M. Issaian, J. A. Kornfield, S. D. Smith, J. T. Grothaus, and M. M. Satkowski, Macromolecules **30**, 7096 (1997).
[15] M. P. Allen and D. J. Tildesley, *Computer Simulation of Liquids* (Clarendon Press, Oxford, 1987).
[16] D. C. Rapaport, *The Art of Molecular Dynamics Simulation* (Cambridge University Press, Cambridge, 1995).
[17] *Molecular-Dynamics Simulation of Statistical Mechanical Systems*, edited by G. Ciccotti, and W. G. Hoover (North-Holland, Amsterdam, 1986).
[18] *Computer Simulation of Polymers*, edited by R. J. Roe (Prentice-Hall, New Jersey, 1991).
[19] *Monte Carlo and Molecular Dynamics Simulations in Polymer Science*, edited by K. Binder (Oxford University Press, New York, 1995).
[20] J. G. E. M. Fraaije, J. Chem. Phys. **99**, 9202 (1993).
[21] J. G. E. M. Fraaije, B. A. C. van Vlimmeren, N. M. Maurits, M. Postma, O. A. Evers, C. Hoffmann, P. Altevogt, and G. Goldbeck-Wood, J. Chem. Phys. **106**, 4260 (1997).
[22] A. V. Zvelindovsky, G. J. A. Sevink, B. A. C. van Vlimmeren, and J. G. E. M. Fraaije, Phys. Rev. E **57**, R4879 (1998).
[23] T. Ohta and K. Kawassaki, Macromolecules **19**, 2621 (1986).
[24] K. Luo and Y. Yang, J. Chem. Phys. **115**, 2818 (2001).
[25] Y. Oono and Y. Shiwa, Mod. Phys. Lett. B **1**, 49 (1987).
[26] Y. Oono and S. Puri, Phys. Rev. A **38**, 434 (1988).
[27] M. Bahiana and Y. Oono, Phys. Rev. A **41**, 6763 (1990).
[28] H. Guo, K. Kremer, and T. Soddemann, Phys. Rev. E **66**, 061503 (2002).
[29] P. J. Hoogerbrugge and J. M. V. A. Koelman, Europhys. Lett. **19**, 155 (1992).
[30] J. M. V. A. Koelman and P. J. Hoogerbrugge, Europhys. Lett. **21**, 363 (1993).
[31] P. Español and P. Warren, Europhys. Lett. **30**, 191 (1995).
[32] R. D. Groot and P. B. Warren, J. Chem. Phys. **107**, 4423 (1997).
[33] T. Soddemann, B. Dünweg, and K. Kremer, Phys. Rev. E **68**, 046702 (2003).
[34] Y. Kong, C. W. Manke, W. G. Madden, and A. G. Schlijper, Int. J. Thermophys. **15**, 1093 (1994).
[35] A. G. Schlijper, P. J. Hoogerbrugge, and C. W. Manke, J. Rheol. **39**, 567 (1995).
[36] R. D. Groot and T. J. Madden, J. Chem. Phys. **108**, 8713 (1998).
[37] A. F. Jakobsen, O. G. Mouritsen, and G. Besold, J. Chem. Phys. **122**, 204901 (2005).
[38] M. P. Allen, J. Phys. Chem. B **110**, 3823 (2006).
[39] M. Revenga, I. Zúñiga, and P. Español, Comput. Phys. Commun. **121-122**, 309 (1999).
[40] E. S. Boek, P. V. Coveney, H. N. W. Lekkerkerker, and P. Schoot, Phys. Rev. E **55**, 3124 (1997).
[41] S. M. Willemsen, H. C. Hoefsloot, P. D. Iedema, and G. Y. Kim, Int. J. Mod. Phys. C **11**, 881 (2000).
[42] A. W. Lees and S. F. Edwards, J. Phys. C **5**, 1921 (1972).
[43] I. Rychkov, Macromol. Theory Simul. **14**, 207 (2005).
[44] H. Guo and K. Kremer, J. Chem. Phys. **118**, 7714 (2003).
[45] M. E. Velázquez and A. Gama-Goicochea, J. Chem. Phys. **124**, 084103 (2006).

[46] I. W. Hamley, J. Phys.: Condens. Matter **13**, R643 (2001).
[47] H. Leist, D. Maring, T. Thurn-Albrecht, and U. Wiesner, J. Chem. Phys. **110**, 8225 (1999).
[48] V. K. Gupta, R. Krishnamoorti, J. A. Kornfield, and S. D. Smith, Macromolecules **28**, 4464 (1995).
[49] P. G. de Gennes and J. Prost, *The Physics of Liquid Crystals* (Clarendon Press, Oxford, 1993).
[50] J. P. Hurault, J. Chem. Phys. **59**, 2086 (1973).
[51] Z. G. Wang, J. Chem. Phys. **100**, 2298 (1994).
[52] H. Wang, P. K. Kesani, N. P. Balsara, and B. Hammouda, Macromolecules **30**, 982 (1997).
[53] M. Imai, K. Nakaya, and T. Kato, Eur. Phys. J. E **5**, 391 (2001).
[54] Th. Soddemann, G. K. Auernhammer, H. Guo, B. Dünweg, and K. Kremer, Eur. Phys. J. E **13**, 141, (2004).
[55] B. Fraser, C. Denniston, and M. H. Müser, J. Polym. Sci., Part B: Polym. Phys. **43**, 970 (2005).
[56] S. J. Singer, Phys. Rev. E **48**, 2796 (1993).
[57] D. J. Read, R. A. Duckett, J. Sweeney, and T. C. B. McLeish, J. Phys. D **32**, 2087 (1999).
[58] G. H. Fredrickson, J. Rheol. **38**, 1045 (1994).
[59] K. Amundson and H. Helfand, Macromolecules **26**, 1324 (1993).